ARTICLE OPEN ACCESS

Brain Regional Differences in Hexanucleotide Repeat Length in X-Linked Dystonia-Parkinsonism Using Nanopore Sequencing

Charles Jourdan Reyes, PhD,* Björn-Hergen Laabs, MSc,* Susen Schaake, BSc, Theresa Lüth, MSc, Raphaela Ardicoglu, MSc, Aleksandar Rakovic, PhD, Karen Grütz, PhD, Daniel Alvarez-Fischer, MD, Roland Dominic Jamora, MD, Raymond L. Rosales, MD, PhD, Imke Weyers, MD, Inke R. König, PhD, Norbert Brüggemann, MD, Christine Klein, MD, Valerija Dobricic, PhD, Ana Westenberger, PhD, and Joanne Trinh, PhD

Correspondence
Dr. Trinh
joanne.trinh@neuro.uni-luebeck.de

Neurol Genet 2021;7:e608. doi:10.1212/NXG.0000000000000608

Abstract

Objective

Our study investigated the presence of regional differences in hexanucleotide repeat number in postmortem brain tissues of 2 patients with X-linked dystonia-parkinsonism (XDP), a combined dystonia-parkinsonism syndrome modified by a $(CCCTCT)_n$ repeat within the causal SINE-VNTR-*Alu* retrotransposon insertion in the *TAF1* gene.

Methods

Genomic DNA was extracted from blood and postmortem brain samples, including the basal ganglia and cortex from both patients and from the cerebellum, midbrain, and pituitary gland from 1 patient. Repeat sizing was performed using fragment analysis, small-pool PCR-based Southern blotting, and Oxford nanopore sequencing.

Results

The basal ganglia ($p < 0.001$) and cerebellum ($p < 0.001$) showed higher median repeat numbers and higher degrees of repeat instability compared with blood.

Conclusions

Somatic repeat instability may predominate in brain regions selectively affected in XDP, thereby hinting at its potential role in disease manifestation and modification.

*These authors contributed equally to this work as co–first authors.

From the Institute of Neurogenetics (C.J.R., S.S., T.L., R.A., A.R., K.G., D.A.-F., N.B., C.K., V.D., A.W., J.T.), University of Lübeck, and Institute of Medical Biometry and Statistics (B.-H.L., I.R.K.), University of Lübeck, Germany; Department of Neurosciences (R.D.J.), College of Medicine–Philippine General Hospital, University of the Philippines Manila; Department of Neurology and Psychiatry (R.L.R.), University of Santo Tomas Hospital, Manila, Philippines; Institute of Anatomy (I.W.), Department of Neurology (N.B.), and Lübeck Interdisciplinary Platform for Genome Analytics (V.D.), University of Lübeck, Germany.

Go to Neurology.org/NG for full disclosures. Funding information is provided at the end of the article.

The Article Processing Charge was funded by the German Research Foundation (DFG).

Glossary

DIG = digoxigenin; **HD** = Huntington disease; **QCD** = quartile coefficients of dispersion; **RN** = repeat number; **SP-PCR** = small-pool PCR; **SVA** = SINE-VNTR-*Alu*; **XDP** = X-linked dystonia-parkinsonism.

X-linked dystonia-parkinsonism (XDP) is an adult-onset neurodegenerative disorder characterized by rapidly progressive dystonia and parkinsonism.[1] Unique to individuals of Filipino descent, XDP is caused by a single founder mutation: a SINE-VNTR-*Alu* (SVA) retrotransposon insertion in the *TAF1* gene.[2,3] This change downregulates the expression of *TAF1*,[4,5] likely leading to basal ganglia degeneration.[6] Consequently, XDP has long been considered a model disorder to study how basal ganglia pathology leads to dystonia and parkinsonism.[6] However, the notion of exclusive striatal atrophy in this movement disorder has been recently challenged by neuroimaging studies proposing that other brain regions such as the cortex and the cerebellum may be affected as well.[7] Of note, patients with XDP exhibit a range of nonmotor features, including cognitive impairment, anxiety, and depression.[8]

Recent studies suggest that XDP shares genetic similarities with microsatellite repeat expansion disorders such as Huntington disease (HD), several forms of spinocerebellar ataxia, and more than 20 other human diseases.[9,10] Namely, it has been reported that the length of the polymorphic $(CCCTCT)_n$ domain within the *TAF1* SVA retrotransposon acts as a genetic modifier of disease expressivity in XDP. The longer the $(CCCTCT)_n$ repeat, the more severe the disease, and the earlier the age at onset.[9,10] The hexanucleotide repeat also showed somatic repeat variability,[10] raising the possibility that higher RNs in specific brain tissues may contribute to selective neurodegeneration. Hence, this study was undertaken to investigate in greater detail whether regional differences in $(CCCTCT)_n$ RN reflect the pattern of neuronal loss seen in XDP.

Methods

Standard Protocol Approvals, Registrations, and Patient Consents

This study was approved by the Ethics Committee of the University of Lübeck, Germany. Postmortem brain samples from the abovementioned patients were used in this investigation in accordance with the "Gesetz über das Leichen-, Bestattungs- und Friedhofswesen (Bestattungsgesetz) des Landes Schleswig-Holstein vom 04.02.2005, Abschnitt II, § 9 (Leichenöffnung, anatomisch)." In this case, it is allowed to dissect the bodies of the patients (Körperspender/in) for scientific and/or educational purposes without explicit prior approval from patients or their legal representatives. The first patient (L-10322) died in the Philippines, and ethics approval was obtained at the Philippine Children's Medical Center, Department of Pathology. The second patient (L-7995) died in Lübeck, Germany, and 2 family members (1 sister and 1 brother) provided written and signed consent with Ethics Committee approval.

Genetic Analyses

To further investigate the link between RN differences and neurodegeneration in XDP, we extracted genomic DNA from blood and postmortem brain samples from 2 affected individuals and performed hexanucleotide repeat sizing with 4 different methods: (1) fragment analysis,[10] (2) small-pool PCR (SP-PCR) coupled with Southern blotting, (3) Cas9-targeted nanopore sequencing, and (4) deep nanopore sequencing of the SVA amplicon. Genomic DNA was extracted using the QIAamp DNA Mini Kit and Blood and Cell Culture DNA Midi Kit (Qiagen, Hilden, Germany) for SP-PCR-based Southern blotting and nanopore sequencing, respectively, following the manufacturer's prescribed procedure. Oxford nanopore sequencing permits the detection of single molecules of DNA without the need for PCR amplification.[11] We thus performed long-read sequencing by enriching the SVA insertion using the Nanopore Cas9-targeted sequencing protocol.[12] Long-read sequencing was applied only to basal ganglia (striatum) and cerebellum samples from L-7995.

SP-PCR–Based Southern Blotting

SP-PCR is an efficient and sensitive method for accurately measuring the heterogeneity of RNs in specific tissues in the absence of artifacts.[13] In brief, 30-mg tissue fragments derived from 2 (cortex and basal ganglia) and 5 (cortex, basal ganglia, cerebellum, pituitary gland, and midbrain) brain regions were dissected from L-10322 and L-7995, respectively. For patient L-10322, DNA from the basal ganglia was isolated from the caudate, anterior putamen, posterior putamen, globus pallidus internus, and globus pallidus externus. For the cortex, DNA from the frontal and temporal cortices was used. Similarly, for patient L-7995, DNA from the basal ganglia was extracted from the striatum, globus pallidus internus, and globus pallidus externus. For the cortex, DNA from the frontal and oculomotor cortices was used.

Brain tissues from these individuals were previously observed to exhibit somatic mosaicism.[10] Hence, for each brain region, 75 pg of genomic DNA derived from ~10 cells was used as template for a previously established long-range PCR reaction amplifying the *TAF1* SVA insertion (eTable 1, links.lww.com/NXG/A435).[14] The said concentration was used to rapidly assess the diversity of RNs per tissue while still avoiding the drawbacks of bulk PCR.[13] Then, PCR products were digested with the restriction enzymes BsaI, HindIII, HaeIII, and MseI (New England Biolabs, Ipswich, MA) to generate a $458 + (n \times 6)$ bp fragment (n = number of repeats) containing the hexanucleotide repeat region and adjacent base

pairs. This digestion mixture was electrophoresed on a denaturing 7% polyacrylamide gel and then transferred to a positively charged nylon membrane (GE Healthcare, Buckinghamshire, United Kingdom) by overnight capillary blotting. After prehybridization, $(AGAGGG)_6$ probes, 3′ labeled with digoxigenin (DIG) using the DIG Oligonucleotide 3′-End Labeling Kit (Roche Applied Science, Mannheim, Germany), were hybridized overnight at 42°C.

All hybridization, washing, and detection procedures were performed following the DIG Application Manual (Roche Applied Science, Mannheim, Germany). The ChemiDoc MP Imaging System (Bio-Rad Laboratories, Hercules, CA) was used for visualizing the chemiluminescent signal. Fragments amplified were sized using custom-made markers containing 30, 35, 40, 45, 50, and 55 hexanucleotide repeats. The marker bands were generated using the aforementioned procedures except that bulk genomic DNA (10 ng) from the previously genotyped patients was used as template. The use of such markers ensured that the hybridization probes were specific to the repeat-bearing fragments and the observed bands with different sizes were not a result of PCR artifacts or DNA degradation.

Oxford Nanopore Sequencing

Customizable crRNAs guided the Cas9 ribonucleoprotein complex to cleave out the region of interest. The resulting blunt ends with 5′ phosphates were used for the specific ligation of the sequencing adapters to the region of interest.[12] Hence, for library preparation, 4 CRISPR–Cas9 crRNAs were designed with the ChopChop online tool[15] (chopchop.cbu.uib.no): 2 upstream (genomic location GRCh38, [target sequence] chrX: 70,657,572 [AAACTTCCCCCGATCCTGCTTGG], chrX: 70,658,413 [GTCCAGTCTACCAAGTAAACAGG]) and 2 downstream (genomic location [target sequence] chrX: 70,660,444 [GACGTAAGTGTGACGACATGGG], chrX: 70,660,445 [TGACGTAAGTGTGACGACA TTGG]) of the SVA insertion (eFigure 1, links.lww.com/NXG/A435). For the Cas9-targeted nanopore sequencing, 4 flow cells (R9.4.1) loaded with 5 libraries (4 × 5 μg and 1 × 1 μg of DNA) were used for blood. Three flow cells (R9.4.1) loaded with 5 libraries (4 × 5 μg and 1 × 10 μg of DNA) were used for the cerebellum. Four flow cells (R9.4.1) loaded with 5 libraries (3 × 3 μg, 1 × 2 μg, and 1 × 1 μg of DNA) were used for the basal ganglia (striatum). In addition, 1 flow cell with 1 μg of barcoded PCR product was run for each tissue. The locations of the guide RNAs used for Cas9-targeted enrichment and the PCR primer for deep nanopore sequencing are shown in eFigure 1. The Cas9 excision resulted in a 5.5-kb product, including the 2.6-kb SVA insertion. The LSK109 ligation sequencing kit (Oxford Nanopore Technologies, Oxford, United Kingdom) was used for library preparation without barcoding, and subsequent sequencing was performed on the R9.4.1 flow cell on the MinION. Base calling was performed with integrated Guppy algorithm in MinKNOW (version 2.2.3) on the MinIT. For Cas9-targeted enrichment, we obtained 148,975 reads on average per sample (blood-derived DNA: 107,138; basal ganglia–derived DNA: 178,449; and cerebellum-derived DNA: 161,284) and 1,630 reads that were mapped to the target with at least 1 kb of alignment length (blood-derived DNA: 1,081; basal ganglia–derived DNA: 1,133; and cerebellum-derived DNA: 2,677). Thus, the proportion of reads that mapped to the target was on average 1.1% per sample.

Separately, a 3.1-kb amplicon product of the SVA was generated with long-range PCR with the use of primers, as previously published.[14] For this 3.1-kb PCR amplicon sequencing, 1 μg of DNA per product was used, and all samples were multiplexed together on 1 flow cell (R9.4.1) with the native barcoding kit (EXP-NBD104). After multiplex barcoding the PCR products, the LSK109 ligation sequencing kit was used for library preparation, and nanopore sequencing was performed with the MinION and the R9.4.1 flow cell. Base calling was performed with integrated Guppy algorithm in MinKNOW (version 2.2.3) on the MinIT.

For the PCR amplicon, the proportion of reads that mapped to the region of interest was larger for the sequenced amplicons that were generated for the deep nanopore sequencing. We obtained 98,883 reads on average per sample (blood-derived DNA: 129,463; basal ganglia–derived DNA: 49,704; and cerebellum-derived DNA: 117,482) and 56,695 reads that were mapped to the target with at least 1 kb of alignment length (blood-derived DNA: 78,438; basal ganglia–derived DNA: 29,725; and cerebellum-derived DNA: 61,923) resulting in a proportion of 57.7%.

To analyze all sequence data with NCRF, the FASTQ files were aligned to the reference (hg19 including the SVA insertion) FASTA file with minimap2 (version 2.17). To extract those reads that were on target, a BAM file was generated that only contained reads that had an alignment length of more than 1 kb with samtools (version 1.3.1). Subsequently, the BAM file was converted to FASTQ format with samtools as well. As NCRF requires the FASTA format as an input, the FASTQ file was converted. To optimize the NCRF analysis, we set the maximum mismatch ratio to 20% and the minimum query length to 108 bp, which equals a repeat count of 18. The script used in this study is available on GitHub (github.com/nanopol/xdp_sva/). Further filtering with the NCRF software tool resulted in 1,137 reads per sample (blood-derived DNA: 721; basal ganglia–derived DNA: 759; and cerebellum-derived DNA: 1,932) for the Cas9-targeted enrichment. After the performed NCRF filtering, 60,589 reads remained (blood-derived DNA: 83,470; basal ganglia–derived DNA: 31,544; and cerebellum-derived DNA: 66,754).

Statistical Analyses

Both Southern blotting and long-read sequencing were used to assess the RNs. We compared RNs derived from different tissues from the respective same individual by statistical tests. RNs per tissue showed deviations from a symmetric normal distribution and had different variances. As a result, the Mood's median test was applied to test whether the median

RNs differ between tissues. To account for multiple comparisons of varying brain tissues with blood, the overall significance level of $\alpha = 0.05$ per patient was split up to $0.05/2 = 0.025$ for patient L-10322 and $0.05/5 = 0.01$ for patient L-7995. Boxplots were used to show the distribution of RNs per tissue, whereas quartile coefficients of dispersions (QCDs) and corresponding 95% confidence intervals were calculated to describe the interquartile range relative to the distribution's median.

Data Availability

The scripts for the Cas9 enrichment and amplicon runs on the nanopore, FASTA files are available on a GitHub repository (github.com/nanopol/xdp_sva/).

Results

Clinical Description of the Patients

The first patient (L-10322), a former seaman, developed first symptoms at age 50 years. At age 56 years, he presented with a parkinsonian phenotype, including drooling, dysphagia, resting tremor of the right hand, and loss of balance when walking. He was treated with clonazepam and biperiden. In addition to XDP, he was diagnosed with pulmonary fibrosis at age 50 years. He died at age 57 years.

The second patient (L-7995), a former customs employee, initially manifested with blepharospasm at age 31 years. Dystonia rapidly progressed in this patient and became generalized within a few years. On neurologic examination, he showed severe generalized dystonia, mostly pronounced in the upper half of the body (the Burke-Fahn-Marsden Dystonia Rating Scale score: 69/120). In addition, he had parkinsonian signs, including limb rigidity, but dystonia was clearly prominent. At age 35 years, he died in a cachexic state from pneumogenic sepsis due to bacterial aspiration pneumonia and concurrent pulmonary tuberculosis.

Genetic Findings

Our standard fragment analysis identified 41 and 45 $(CCCTCT)_n$ repeats in the blood-derived DNA from L-10322 and L-7995, respectively. However, the SP-PCR–based Southern blot analysis revealed heterogeneity across RNs in all tissues examined from both individuals (Figure 1A). In particular, median RNs were significantly higher in the basal ganglia (RN = 42.56, $p = 4 \times 10^{-7}$) and cortex (RN = 42.85, $p = 1.83 \times 10^{-4}$) compared with blood (RN = 39.94) from L-10322 (Figure 1B). This observation was consistent with RN counts in L-7995, who also exhibited higher median RNs in the aforementioned brain regions (RN = 46.98, $p = 4.31 \times 10^{-4}$ and RN = 46.78, $p = 4.67 \times 10^{-4}$ for the basal ganglia and cortex, respectively) compared with blood (RN = 45.30) (Figure 1C). Furthermore, although no significant difference in median RNs was observed between the other brain areas and blood from L-7995, a slight tendency toward higher median RNs was found in the cerebellum (RN = 45.67) and midbrain (RN = 46.54). These findings were consistent with the results of nanopore sequencing after Cas9 enrichment for L-7995. With Cas9-targeted enrichment and nanopore sequencing, we obtained >700 single-molecule reads for each sample type. This also showed higher median RNs in the basal ganglia (RN = 46.8, $p < 0.0001$) and cerebellum (RN = 45.8, $p = 0.0002$) compared with blood (RN = 45.2) for L-7995 (Figure 1D). In addition, long-read deep sequencing of the amplicon encompassing the SVA detected n > 31,000 single-molecule reads for each tissue type and also showed higher median RNs in the basal ganglia (RN = 49.3, $p < 0.0001$) and cerebellum (RN = 49.0, $p < 0.0001$) compared with blood (RN = 48.2) (Figure 1E).

Correspondingly, based on Southern blotting, the basal ganglia and cortex showed higher QCDs (QCD = 0.060 and QCD = 0.062, respectively) compared with blood in L-10322 (QCD = 0.044) (Figure 1F), whereas all brain regions, except the midbrain (QCD = 0.026), exhibited higher QCDs compared with blood (QCD = 0.026) in L-7995 (Figure 1G). Cas9-targeted sequencing also showed higher QCD for the basal ganglia (QCD = 0.080) compared with blood in L-7995 (QCD = 0.077) (Figure 1H). However, the cerebellum had a lower QCD (QCD = 0.070) compared with blood. The PCR amplicons and deep sequencing showed higher QCD for the basal ganglia and cerebellum compared with blood (QCD = 0.070, 0.063, and 0.062, respectively) (Figure 1I).

Discussion

In addition to significant striatal volume loss in the basal ganglia,[6] patients with XDP show gray matter volume loss in the cerebellum and a mild reduction in cortical thickness that has been linked to cognitive dysfunction.[7] Thus, it is remarkable that in our study, both the basal ganglia and the cortex showed higher median RNs and higher degrees of repeat instability compared with blood in the 2 patients based on SP-PCR-based Southern blotting. Nanopore-based long-read sequencing also detected a similar tendency of the repeats to expand in the basal ganglia and the cerebellum of 1 patient. In HD, the brain regions that exhibited the most evident neuropathology were also reported to have the most pronounced mosaicism.[16] Thus, our finding of the presence of higher median RNs in the basal ganglia, cortex, and cerebellum may suggest a role for somatic mosaicism in disease manifestation and modification. In keeping with this notion, somatic repeat instability in the cortex was found to be an age at onset modifier in HD.[17] Furthermore, genetic and pharmacologic inhibition of somatic repeat expansions significantly delays disease onset and rescues progressive motor dysfunction in a transgenic mouse model of HD.[18]

Our approach to analyze somatic repeat instability in different tissues entailed a number of technical limitations. First, 75 pg of genomic DNA was used as template to rapidly evaluate the diversity of RNs per tissue.[13] However, in the Southern blots, the empirical determination of average number of amplifiable

Figure 1 Number and Instability of $(CCCTCT)_n$ Repeats in Blood and Different Brain Regions

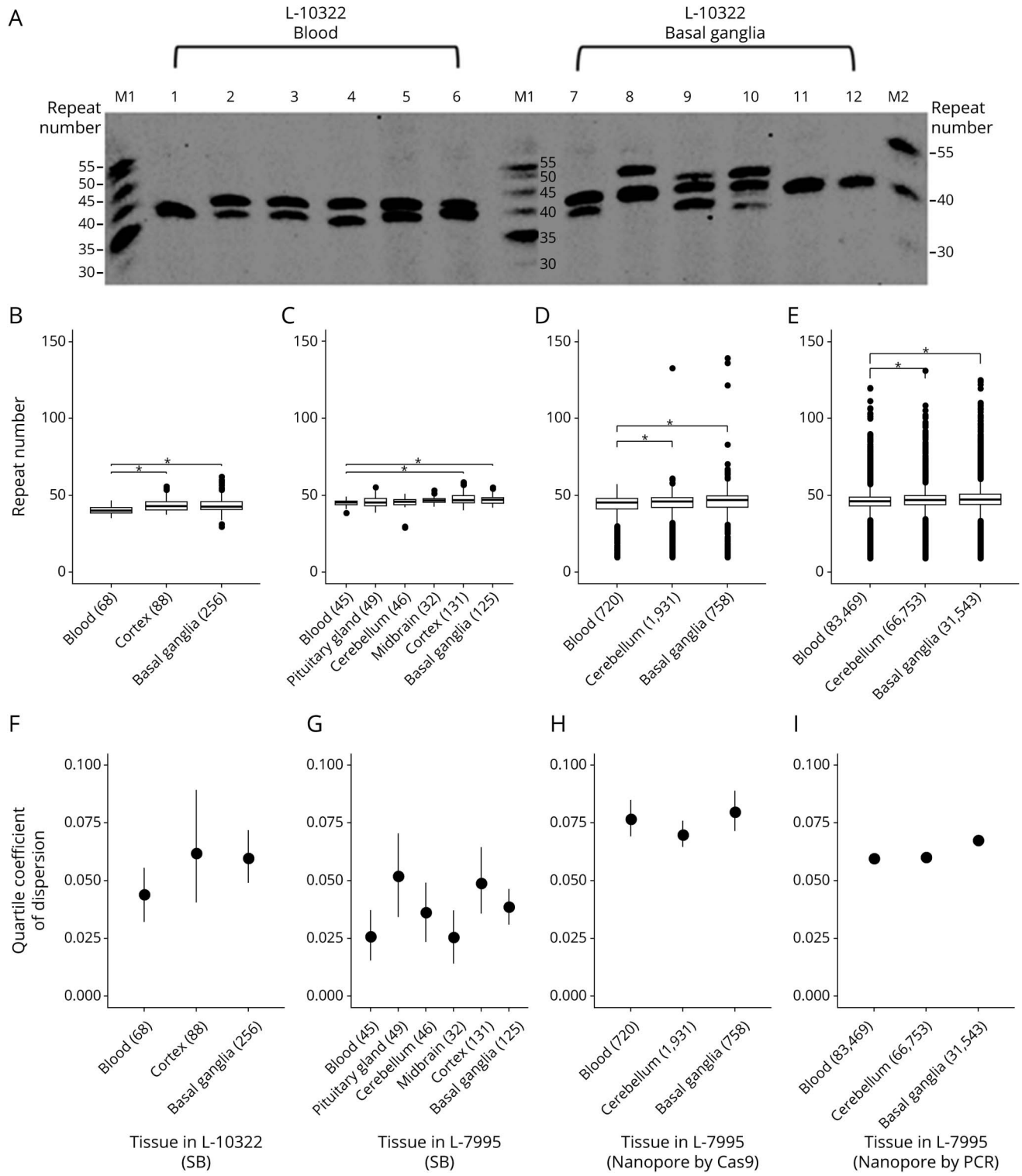

(A) Representative Southern blot image illustrating repeat number (RN) heterogeneity in the blood (lanes 1–6) and basal ganglia (lanes 7–12) of L-10322. Each lane represents 1 small-pool PCR reaction using DNA from the corresponding tissue as template. Custom-made size markers in lanes M1 and M2 show the sizes of alleles in RNs. Boxplots showing median RNs for (B) L-10322 and (C) L-7995 measured using Southern blotting (SB) and (D) L-7995 with Oxford Nanopore long-read sequencing after Cas9 enrichment (E) L-7995 measured with PCR amplification of the SVA and subsequent Oxford Nanopore deep long-read sequencing. Forest plots presenting repeat instability measured as the quartile coefficient of dispersion (QCD) in (F) L-10322 and (G) L-7995 based on SB and (H) L-7995 with Nanopore sequencing with Cas9 enrichment (I) L-7995 with Nanopore sequencing of PCR product. Parentheses indicate the number of bands or alleles measured for each tissue. Asterisks indicate significant differences between samples.

molecules for each sample (i.e., calculation of genome equivalents) was not performed, which affects the estimation of degree of somatic instability. Nevertheless, we used long-read sequencing to detect single molecules.[12] From this analysis, we obtained the same median RN as Southern blot analysis with the Cas9-targeted enrichment. Deep amplicon-based sequencing was performed to further validate the repeat expansion in the brain tissue, while considering the caveat of preferential amplification during PCR. Still, the range in RNs was striking and more variable than Southern blot data (eFigure 2, links.lww.com/NXG/A435), likely due to noise from the raw squiggles.[19–21] The accuracy of nanopore sequencing can be hampered by errors from indels and homopolymers.[19] As better bioinformatic tools and training mechanisms are developed over time, the accuracy of long-read sequencing technologies will improve. In fact, nanopore sequencing has already been used to investigate the size and methylation status of unstable microsatellite repeat expansions.[20,22,23] The robustness of our findings is strengthened by the simultaneous comparison between Southern blotting and nanopore sequencing on the *TAF1* SVA hexanucleotide repeat in XDP patients.

In conclusion, our work extends the utility of long-read sequencing to repeat instability, helping us provide further evidence of brain region–specific instability of the $(CCCTCT)_n$ repeat in XDP. Our study of 2 independently analyzed patients is currently unable to determine the exact contribution of somatic repeat expansions to the characteristic pattern of neuronal death seen in XDP. Nevertheless, our work indicates that somatic mosaicism may predominate in brain regions selectively affected in the disease, thereby hinting at its vital role in modifying the yet-unresolved, repeat-mediated pathogenic process leading to neurodegeneration. This finding holds possible translational significance as it highlights the potential of somatic repeat instability as a viable therapeutic target for this emerging repeat expansion disorder.

Acknowledgment

The authors acknowledge Dr. Lillian V. Lee, Dr. Madelyn Pascual, Dr. Mark Angelo C. Ang, Dr. Aloysius Domingo, Dr. Ivy Lique, Dr. Edwin Muñoz, Atty. Geraldine Acuña-Sunshine, and the Sunshine Care Foundation for referral of patients and clinical information. They also thank Ms. Heike Pawlack for the technical assistance.

Study Funding

The study was supported by the Deutsche Forschungsgemeinschaft (DFG FOR2488; to A.R., I.R.K., N.B., A.W., C.K., and J.T.), by funding by the Collaborative Center for X-linked Dystonia-Parkinsonism at Massachusetts General Hospital (to N.B. and C.K.), the Else-Kröner Fresenius Foundation (to N.B. and J.T.), by intramural funds from the University of Lübeck (to C.K. and J.T.), career development award from Peter Engelhorn Foundation (to J.T.), and by a career development award from the Hermann and Lilly Schilling Foundation (to C.K.). C.J. Reyes is supported by a PhD scholarship from the Katholischer Akademischer Ausländer-Dienst.

Disclosure

The authors report no disclosures relevant to the manuscript. Go to Neurology.org/NG for full disclosures.

Publication History

Received by *Neurology: Genetics* February 8, 2021. Accepted in final form June 3, 2021.

Appendix Authors

Name	Location	Contribution
Charles Jourdan Reyes, PhD	University of Lübeck, Germany	Contributed to the conception and design of the study and to the acquisition, analysis, and interpretation of data; participated in drafting the manuscript; and approved its final version
Björn-Hergen Laabs, MSc	University of Lübeck, Germany	Contributed to the statistical analysis and interpretation of data; participated in drafting the manuscript; and approved its final version
Susen Schaake, BSc	University of Lübeck, Germany	Contributed to the acquisition and analysis of data; revised the manuscript for intellectual content; and approved its final version
Theresa Lüth, MSc	University of Lübeck, Germany	Contributed to the acquisition and analysis of data; participated in drafting the manuscript for intellectual content; and approved its final version
Raphaela Ardicoglu, MSc	University of Lübeck, Germany	Contributed to the acquisition and analysis of data; revised the manuscript for intellectual content; and approved its final version
Aleksandar Rakovic, PhD	University of Lübeck, Germany	Contributed to the acquisition and analysis of data; revised the manuscript for intellectual content; and approved its final version
Karen Grütz, PhD	University of Lübeck, Germany	Contributed to the interpretation of data; revised the manuscript for intellectual content; and approved its final version
Daniel Alvarez-Fischer, MD	University of Lübeck, Germany	Contributed to the acquisition and analysis of data; revised the manuscript for intellectual content; and approved its final version
Roland Dominic Jamora, MD	University of the Philippines Manila	Contributed to the acquisition and analysis of data; revised the manuscript for intellectual content; and approved its final version
Raymond L. Rosales, MD, PhD	University of Santo Tomas Hospital, Manila, Philippines	Contributed to the acquisition and analysis of data; revised the manuscript for intellectual content; and approved its final version

Appendix *(continued)*

Name	Location	Contribution
Imke Weyers, MD	University of Lübeck, Germany	Contributed to the acquisition and analysis of data; revised the manuscript for intellectual content; and approved its final version
Inke R. König, PhD	University of Lübeck, Germany	Contributed to the statistical analysis and interpretation of data; revised the manuscript for intellectual content; and approved its final version
Norbert Brüggemann, MD	University of Lübeck, Germany	Contributed to the design of the study and to the acquisition, analysis, and interpretation of data; participated in drafting the manuscript; and approved its final version
Christine Klein, MD	University of Lübeck, Germany	Contributed to the conception and design of the study and to the interpretation of data; revised the manuscript for intellectual content; and approved its final version
Valerija Dobricic, PhD	University of Lübeck, Germany	Contributed to the conception and design of the study and to the analysis and interpretation of data; revised the manuscript for intellectual content; and approved its final version
Ana Westenberger, PhD	University of Lübeck, Germany	Contributed to the conception and design of the study and to the analysis and interpretation of data; participated in drafting the manuscript; and approved its final version
Joanne Trinh, PhD	University of Lübeck, Germany	Contributed to the design of the study and to the acquisition, analysis, and interpretation of data; participated in drafting the manuscript for intellectual content; and approved its final version

References

1. Lee LV, Rivera C, Teleg RA, et al. The unique phenomenology of sex-linked dystonia parkinsonism (XDP, DYT3, 'Lubag'). *Int J Neurosci*. 2011;121(suppl 1):3-11.
2. Domingo A, Westenberger A, Lee LV, et al. New insights into the genetics of X-linked dystonia-parkinsonism (XDP, DYT3). *Eur J Hum Genet*. 2015;23(10):1334-1340.
3. Makino S, Kaji R, Ando S, et al. Reduced neuron-specific expression of the TAF1 gene is associated with X-linked dystonia-parkinsonism. *Am J Hum Genet*. 2007;80(3):393-406.
4. Aneichyk T, Hendriks WT, Yadav R, et al. Dissecting the causal mechanism of X-linked dystonia-parkinsonism by integrating genome and transcriptome assembly. *Cell*. 2018;172(5):897-909.e21.
5. Rakovic A, Domingo A, Grütz K, et al. Genome editing in induced pluripotent stem cells rescues TAF1 levels in X-linked dystonia-parkinsonism. *Mov Disord*. 2018;33(7):1108-1118.
6. Goto S, Lee LV, Munoz EL, et al. Functional anatomy of the basal ganglia in X-linked recessive dystonia-parkinsonism. *Ann Neurol*. 2005;58(1):7-17.
7. Hanssen H, Heldmann M, Prasuhn J, et al. Basal ganglia and cerebellar pathology in X-linked dystonia-parkinsonism. *Brain*. 2018;141(10):2995-3008.
8. Jamora RDG, Ledesma LK, Domingo A, Cenina ARF, Lee LV. Nonmotor features in sex-linked dystonia parkinsonism. *Neurodegener Dis Manag*. 2014;4(3):283-289.
9. Bragg DC, Mangkalaphiban K, Vaine CA, et al. Disease onset in X-linked dystonia-parkinsonism correlates with expansion of a hexameric repeat within an SVA retrotransposon in TAF1. *Proc Natl Acad Sci USA*. 2017;114(51):E11020-E11028.
10. Westenberger A, Reyes CJ, Saranza G, et al. A hexanucleotide repeat modifies expressivity of X-linked dystonia parkinsonism. *Ann Neurol*. 2019;85(6):812-822.
11. Ameur A, Kloosterman WP, Hestand MS. Single-molecule sequencing: towards clinical applications. *Trends Biotechnol*. 2019;37(1):72-85.
12. Gilpatrick T, Lee I, Graham JE, et al. Targeted nanopore sequencing with Cas9-guided adapter ligation. *Nat Biotechnol*. 2020;38(4):433-438.
13. Gomes-Pereira M, Bidichandani SI, Monckton DG. Analysis of unstable triplet repeats using small-pool polymerase chain reaction. *Methods Mol Biol*. 2004;277:61-76.
14. Kawarai T, Pasco PMD, Teleg RA, et al. Application of long-range polymerase chain reaction in the diagnosis of X-linked dystonia-parkinsonism. *Neurogenetics*. 2013;14(2):167-169.
15. Labun K, Montague TG, Krause M, Torres Cleuren YN, Tjeldnes H, Valen E. CHOPCHOP v3: expanding the CRISPR web toolbox beyond genome editing. *Nucleic Acids Res*. 2019;47(W1):W171-W174.
16. Telenius H, Kremer B, Goldberg YP, et al. Somatic and gonadal mosaicism of the Huntington disease gene CAG repeat in brain and sperm. *Nat Genet*. 1994;6(4):409-414.
17. Swami M, Hendricks AE, Gillis T, et al. Somatic expansion of the Huntington's disease CAG repeat in the brain is associated with an earlier age of disease onset. *Hum Mol Genet*. 2009;18(16):3039-3047.
18. Budworth H, Harris FR, Williams P, et al. Suppression of somatic expansion delays the onset of pathophysiology in a mouse model of Huntington's disease. *PLoS Genet*. 2015;11(8):1-22.
19. Harris RS, Cechova M, Makova KD. Noise-cancelling repeat finder: uncovering tandem repeats in error-prone long-read sequencing data. *Bioinformatics*. 2019;35(22):4809-4811.
20. Giesselmann P, Brändl B, Raimondeau E, et al. Analysis of short tandem repeat expansions and their methylation state with nanopore sequencing. *Nat Biotechnol*. 2019;37(12):1478-1481.
21. Logsdon GA, Vollger MR, Eichler EE. Long-read human genome sequencing and its applications. *Nat Rev Genet*. 2020;21(10):597-614.
22. Ebbert MTW, Farrugia SL, Sens JP, et al. Long-read sequencing across the C9orf72 'GGGGCC' repeat expansion: implications for clinical use and genetic discovery efforts in human disease. *Mol Neurodegener*. 2018;13(1):46.
23. De Roeck A, Duchateau L, Van Dongen J, et al. An intronic VNTR affects splicing of ABCA7 and increases risk of Alzheimer's disease. *Acta Neuropathol*. 2018;135(6):827-837.